Lowest order methods for diffusive problems on general meshes

Daniele A. Di Pietro

IFP Energies nouvelles, dipietrd@ifpen.fr

Finite Volumes for Complex Applications VI
Prague, June 8th 2011

Motivations

One key to the success of the finite element method, as developed in engineering practice, was the systematic way that computer codes could be implemented.

S. C. Brenner & L. R. Scott

Essential bibliography

- Multi-point finite volume methods
  - [Aavatsmark *et al.*, 1994–]
  - [Edwards *et al.*, 1994–]
- Mimetic finite difference methods
  - [Brezzi, Lipnikov, Shashkov, Simoncini, 2005–06]
  - [Beirão da Vega, Boffi, Buffa, Kuznetsov, Manzini, *et al.*]
- Variational finite volume methods
  - [Eymard, Gallouët, Herbin, 2000–2011]
  - [Agélas, Droniou, Guichard, Latché, Masson, *et al.*]
- Cell centered and discontinuous Galerkin methods
  - [DP, 2010-11]
  - [Ern & Guermond, 2006–08], [DP & Ern, 2008–2011]
- Domain-specific languages
  - [Prud'homme 2006–11]
  - [DP & Veneziani, 2009]

Outline

General meshes

Formulation based on incomplete polynomial spaces

Implementation

Application to the incompressible Navier–Stokes equations

Outline

General meshes

Formulation based on incomplete polynomial spaces

Implementation

Application to the incompressible Navier–Stokes equations

General meshes I

- Avoid remeshing (e.g. in subsoil modeling)
- Improve domain/solution fitting
- Improve performance (fewer DOFs, reduced fill-in)
- Nonconforming/aggregative mesh adaptivity

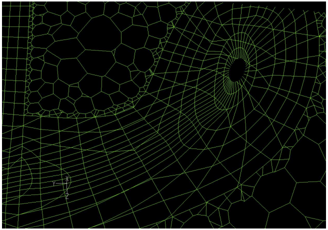

Figure: Near wellbore mesh. See Cindy Guichard on Friday

General meshes II

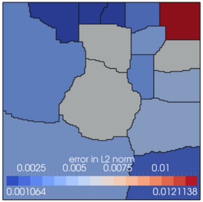

(a) 15 elements

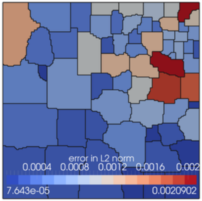

(b) 63 elements

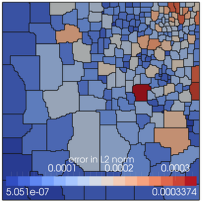

(c) 250 elements

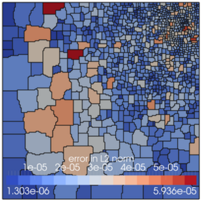

(d) 1024 elements

Figure: Adaptive aggregation [Bassi, Botti, Colombo, DP, & Tesini, 2011]

Admissible mesh sequences for h-convergence I

- Let $\Omega \subset \mathbb{R}^d$ be an open connected bounded polyhedral domain
- Let $(\mathcal{T}_h)_{h\in\mathcal{H}}$ be a sequence of refined meshes of Ω with $h \to 0$
- Polyhedral elements and nonmatching interfaces admitted

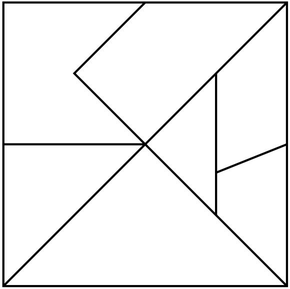

Figure: Example of a polygonal mesh $\mathcal{T}_h$

Admissible mesh sequences for h-convergence II

Trace and inverse inequalities

- Every $\mathcal{T}_h$ admits a simplicial submesh $\mathfrak{S}_h$
- $(\mathfrak{S}_h)_{h\in\mathcal{H}}$ is shape-regular in the sense of Ciarlet
- Every simplex $S \subset T$ is s.t. $h_S \approx h_T$

Optimal polynomial approximation (for error estimates)

Every element T is star-shaped w.r.t. a ball of diameter $\delta_T \approx h_T$

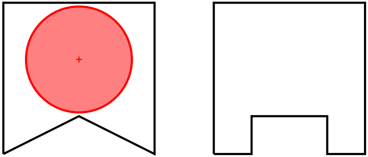

Figure: Admissible (*left*) and non-admissible (*right*) mesh elements

Admissible mesh sequences for h-convergence III

Cell centers

There exists a set of points $(\mathbf{x}_T)_{T \in \mathcal{T}_h}$ s.t.

- all $T \in \mathcal{T}_h$ is star-shaped w.r.t. $\mathbf{x}_T$
- for all $T \in \mathcal{T}_h$, and all $F \in \mathcal{F}_T$, $\mathrm{dist}(\mathbf{x}_T, F) \approx h_T$

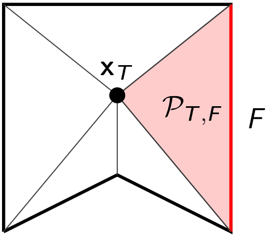

$\mathcal{P}_{T,F}$ = open pyramid of base F and apex $\mathbf{x}_T$

Auxiliary mesh $\mathcal{S}_h$

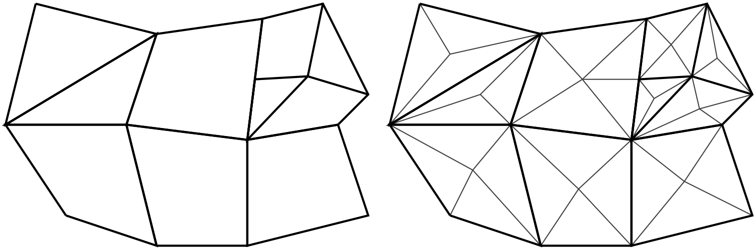

(a) Mesh $\mathcal{T}_h$ (b) Pyramidal submesh $\mathcal{P}_h$

Figure: Choices for $\mathcal{S}_h$

$$\mathcal{S}_h = \mathcal{T}_h \quad \text{or} \quad \mathcal{S}_h = \mathcal{P}_h$$

Spaces $\mathbb{P}_d^k$ and trace operators

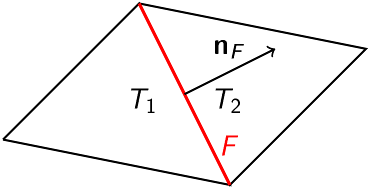

- For $k \geqslant 0$ we define the broken polynomial spaces

$$\mathbb{P}_d^k(\mathcal{S}_h) := \{v \in L^2(\Omega) \,|\, \forall S \in \mathcal{S}_h,\ v_{|S} \in \mathbb{P}_d^k(S)\}$$

- For $F \subset \partial T_1 \cap \partial T_2$ we define the trace operators

$$\text{jump: } [\![v]\!] := v_{|T_1} - v_{|T_2}, \qquad \text{average: } \{v\} := \frac{1}{2}\left(v_{|T_1} + v_{|T_2}\right)$$

Lowest order methods (for industrial applications)

- The choice of a method is application dependent
- Relevant tradeoffs
  - efficiency vs. robustness vs. accuracy vs. cost
  - memory vs. CPU consumption
  - sequential vs. parallel efficiency
- Interest of `FreeFEM`-like platforms but...
- ...multi-purpose libraries need a systematic approach

Lowest order methods as (Petrov)–Galerkin methods based on incomplete polynomial spaces

Beneficial side effects in the analysis

Incomplete broken polynomial spaces

(1) Fix the space of DOFs, e.g.,

$$\text{cell centered: } \mathbb{V}_h = \mathbb{R}^{\mathcal{T}_h} \quad \text{or} \quad \text{hybrid: } \mathbb{V}_h = \mathbb{R}^{\mathcal{T}_h} \times \mathbb{R}^{\mathcal{F}_h}$$

(2) Reconstruct a piecewise constant gradient on $\mathcal{S}_h \in \{\mathcal{T}_h, \mathcal{P}_h\}$

$$\mathfrak{G}_h : \mathbb{V}_h \to [\mathbb{P}_d^0(\mathcal{S}_h)]^d$$

(3) Let $\mathfrak{R}_h : \mathbb{V}_h \to \mathbb{P}_d^1(\mathcal{S}_h)$ be s.t., for all $\mathbf{v}_h \in \mathbb{V}_h$, $S \in \mathcal{S}_h$, $S \subset T$,

$$\mathfrak{R}_h(\mathbf{v}_h)_{|S}(\mathbf{x}) = v_T + \mathfrak{G}_h(\mathbf{v}_h)_{|S} \cdot (\mathbf{x} - \mathbf{x}_T)$$

Use as a trial/test space the incomplete broken polynomial space

$$\mathfrak{R}_h(\mathbb{V}_h) \subset \mathbb{P}_d^1(\mathcal{S}_h)$$

Outline

General meshes

Formulation based on incomplete polynomial spaces

- The MPFA G-method
- The SUSHI method
- The SWIP-ccG method

Implementation

Application to the incompressible Navier–Stokes equations

Model problem

$$-\nabla\cdot(\boldsymbol{\kappa}\nabla u) = f \text{ in } \Omega, \qquad u = 0 \text{ on } \partial\Omega$$

- $\boldsymbol{\kappa}$ is s.p.d. and there is a partition P_Ω s.t.

$$\boldsymbol{\kappa} \in \mathbb{P}_d^0(P_\Omega)^{d,d}$$

- For all $h \in \mathcal{H}$, $\mathcal{T}_h$ is compatible with P_Ω

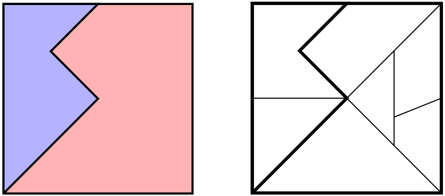

Figure: Partition P_Ω (*left*) and compatible mesh (*right*)

The L-construction

$$\boxed{\mathbb{R}^{\mathcal{T}_h} \ni \mathbf{v}_h \mapsto \xi^{\mathfrak{g}}_{\mathbf{v}_h}}$$

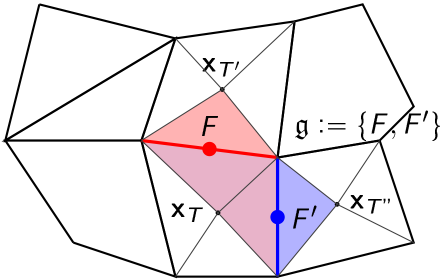

- $\xi^{\mathfrak{g}}_{\mathbf{v}_h}$ is piecewise affine and $\xi^{\mathfrak{g}}_{\mathbf{v}_h}(\mathbf{x}_K) = v_K$ for all $K \in \{T, T', T''\}$
- $\xi^{\mathfrak{g}}_{\mathbf{v}_h}$ is continuous and has continuous diffusive flux across F and F'
- See [Aavatsmark, Eigestad, Mallison, & Nordbotten, 2008]

The MPFA G-method I

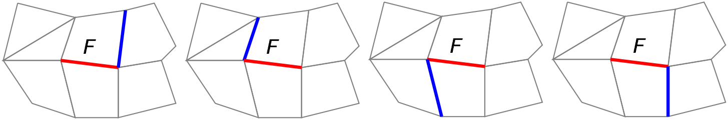

Figure: $\mathcal{G}_F = \{$Faces sharing an element and a node with $F\}$

The flux Φ_F through F is a convex linear combination of subfluxes

$$\forall \mathbf{v}_h \in \mathbb{V}_h, \quad \Phi_F(\mathbf{v}_h) := \sum_{\mathfrak{g} \in \mathcal{G}_F} \varsigma_{\mathfrak{g},F} (\boldsymbol{\kappa} \nabla \xi_{\mathbf{v}_h}^{\mathfrak{g}})_{|T} \cdot \mathbf{n}_F$$

with $\sum_{\mathfrak{g} \in \mathcal{G}_F} \varsigma_{\mathfrak{g},F} = 1$. See [Agélas, DP, & Droniou, 2010]

The MPFA G-method II

(1) Let

$$\mathcal{S}_h^{\mathrm{g}} = \mathcal{P}_h \quad \text{and} \quad \mathbb{V}_h^{\mathrm{g}} = \mathbb{R}^{\mathcal{T}_h}$$

(2) Let for all $\mathbf{v}_h \in \mathbb{V}_h^{\mathrm{g}}$, all $T \in \mathcal{T}_h$, and all $F \in \mathcal{F}_T$,

$$\mathfrak{G}_h^{\mathrm{g}}(\mathbf{v}_h)_{|\mathcal{P}_{T,F}} = \sum_{\mathfrak{g} \in \mathcal{G}_F} \varsigma_{\mathfrak{g},F} \nabla \xi_{\mathbf{v}_h}^{\mathfrak{g}}{}_{|\mathcal{P}_{T,F}}$$

(3) Let $\mathfrak{R}_h^{\mathrm{g}}$ be s.t. for all $\mathbf{v}_h \in \mathbb{V}_h^{\mathrm{g}}$, all $T \in \mathcal{T}_h$, and all $F \in \mathcal{F}_T$,

$$\mathfrak{R}_h^{\mathrm{g}}(\mathbf{v}_h)_{|\mathcal{P}_{T,F}}(\mathbf{x}) = v_T + \mathfrak{G}_h^{\mathrm{g}}(\mathbf{v}_h)_{|\mathcal{P}_{T,F}} \cdot (\mathbf{x} - \mathbf{x}_T)$$

The corresponding discrete space is $V_h^{\mathrm{g}} := \mathfrak{R}_h^{\mathrm{g}}(\mathbb{V}_h^{\mathrm{g}})$

The MPFA G-method III

Find $u_h \in V_h^{\mathrm{g}}$ s.t. for all $v_h \in \mathbb{P}_d^0(\mathcal{T}_h)$

$$-\sum_{F \in \mathcal{F}} \int_F \{\boldsymbol{\kappa} \nabla_h u_h\} \cdot \mathbf{n}_F [\![v_h]\!] = \int_\Omega f v_h$$

Convergence [Agélas, DP, & Droniou, 2010]

Assuming that at least one L-construction exists for each face, the sequence of discrete solutions converges to u in $L^q(\Omega)$ for $q \in [1, {}^{2d}/_{d-2})$. A strongly convergent gradient also exists.

Small footprint but well-posedness only under strict assumptions
$\Longrightarrow$ gradient schemes

A gradient reconstruction based on Green's formula

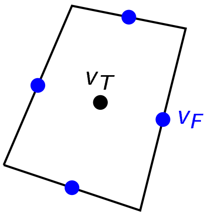

- Let $(\mathbf{v}_h^{\mathcal{T}}, \mathbf{v}_h^{\mathcal{F}}) \in \mathbb{V}_h^{\text{hyb}} := \mathbb{R}^{\mathcal{T}_h} \times \mathbb{R}^{\mathcal{F}_h}$. For all $T \in \mathcal{T}_h$,

$$\boxed{\mathfrak{G}_h^{\text{grn}}(\mathbf{v}_h^{\mathcal{T}}, \mathbf{v}_h^{\mathcal{F}})_{|T} = \frac{1}{|T|_d} \sum_{F \in \mathcal{F}_T} |F|_{d-1} (v_F - v_T)\mathbf{n}_{T,F}}$$

- The L^2-norm of $\mathfrak{G}_h^{\text{grn}}$ is not a norm on general meshes
- See [Eymard, Gallouët, Herbin, 2004]

Stabilization using residuals

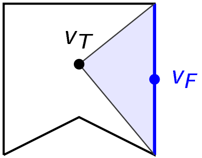

- Following [Eymard, Gallouët, & Herbin, 2009] define

$$\mathfrak{r}_h(\mathbf{v}_h^{\mathcal{T}}, \mathbf{v}_h^{\mathcal{F}})_{|\mathcal{P}_{T,F}} = \frac{\sqrt{d}}{d_{T,F}} \left[v_F - \left(v_T + \mathfrak{G}_h^{\text{grn}}(\mathbf{v}_h^{\mathcal{T}}, \mathbf{v}_h^{\mathcal{F}}) \cdot (\overline{\mathbf{x}}_F - \mathbf{x}_T) \right) \right] \mathbf{n}_{T,F}$$

- We introduce the stabilized gradient

$$\boxed{\mathfrak{G}_h^{\text{hyb}}(\mathbf{v}_h^{\mathcal{T}}, \mathbf{v}_h^{\mathcal{F}}) = \mathfrak{G}_h^{\text{grn}}(\mathbf{v}_h^{\mathcal{T}}, \mathbf{v}_h^{\mathcal{F}}) + \mathfrak{r}_h(\mathbf{v}_h^{\mathcal{T}}, \mathbf{v}_h^{\mathcal{F}})}$$

The L^2-norm of $\mathfrak{G}_h^{\text{hyb}}$ is a norm on general polyhedral meshes

The SUSHI scheme with hybrid unknowns I

Find $u_h \in V_h^{\text{hyb}}$ with $V_h^{\text{hyb}} \subset \mathbb{P}_d^1(\mathcal{P}_h)$ defined from $\mathfrak{G}_h^{\text{hyb}}$ s.t.

$$\int_\Omega \boldsymbol{\kappa}\nabla_h u_h \cdot \nabla_h v_h = \int_\Omega f v_h \quad \forall v_h \in V_h^{\text{hyb}}$$

Convergence [Eymard, Gallouët, & Herbin, 2009]

Let $(u_h)_{h\in\mathcal{H}}$ denote the sequence of discrete solutions on the admissible mesh family $(\mathcal{T}_h)_{h\in\mathcal{H}}$. Then, $P_0 u_h \to u$ in $L^2(\Omega)$ and $\nabla_h u_h \to u$ in $L^2(\Omega)^d$.

Generalization of the Crouzeix–Raviart FE to non-simplicial meshes

Reducing the unkowns: Trace interpolation

$$\boxed{\text{hybrid:} \quad \mathfrak{G}_h^{\text{hyb}}(\mathbf{v}_h^{\mathcal{T}}, \mathbf{v}_h^{\mathcal{F}})}$$

- The vector $\mathbf{v}_h^{\mathcal{F}}$ can be interpolated using the L-construction

$$\mathbf{v}_h^{\mathcal{F}} = \mathbf{T}_h(\mathbf{v}_h^{\mathcal{T}}) := (\xi_{\mathbf{v}_h}^{\mathfrak{g}_F}(\overline{\mathbf{x}}_F))_{F \in \mathcal{F}_h}$$

- This choice honors the heterogeneity of $\boldsymbol{\kappa}$
- $\mathfrak{g}_F \in \mathcal{G}_F$ is the L-group with the best approximation properties

$$\boxed{\text{cell centered:} \quad \mathfrak{G}_h^{\text{cc}}(\mathbf{v}_h^{\mathcal{T}}) := \mathfrak{G}_h^{\text{hyb}}(\mathbf{v}_h^{\mathcal{T}}, \mathbf{T}_h(\mathbf{v}_h^{\mathcal{T}}))}$$

The SWIP-ccG method I

(1) We consider an alternative inspired by dG methods. Let

$$\boxed{\mathcal{S}_h^{\text{ccg}} = \mathcal{T}_h \quad \text{and} \quad \mathbb{V}_h^{\text{ccg}} = \mathbb{R}^{\mathcal{T}_h}}$$

(2) Let for all $\mathbf{v}_h \in \mathbb{V}_h^{\text{ccg}}$

$$\boxed{\mathfrak{G}_h^{\text{ccg}}(\mathbf{v}_h) := \mathfrak{G}_h^{\text{grn}}(\mathbf{v}_h, \mathbf{T}_h(\mathbf{v}_h))}$$

(3) Let $\mathfrak{R}_h^{\text{ccg}}$ be s.t. for all $\mathbf{v}_h \in \mathbb{V}_h^{\text{ccg}}$ and all $T \in \mathcal{T}_h$,

$$\boxed{\mathfrak{R}_h^{\text{ccg}}(\mathbf{v}_h)_{|T}(\mathbf{x}) = v_T + \mathfrak{G}_h^{\text{ccg}}(\mathbf{v}_h)_{|T} \cdot (\mathbf{x} - \mathbf{x}_T)}$$

The corresponding discrete space is $V_h^{\text{ccg}} := \mathfrak{R}_h^{\text{g}}(\mathbb{V}_h^{\text{ccg}})$

The SWIP-ccG method II

Find $u_h \in V_h^{\mathrm{ccg}}$ s.t. for all $v_h \in V_h^{\mathrm{ccg}}$

$$a_h^{\mathrm{ccg}}(u_h, v_h) = \int_\Omega f v_h$$

with

$$a_h^{\mathrm{ccg}}(u_h, v_h) = \int_\Omega \boldsymbol{\kappa} \nabla_h u_h \cdot \nabla_h v_h + \sum_{F \in \mathcal{F}_h} \frac{\gamma_F}{h_F} \eta \int_F [\![u_h]\!] [\![v_h]\!] - \sum_{F \in \mathcal{F}_h} \int_F \left[\{\boldsymbol{\kappa} \nabla_h u_h\}_\omega \cdot \mathbf{n}_F [\![v_h]\!] + [\![u_h]\!] \{\boldsymbol{\kappa} \nabla_h v_h\}_\omega \cdot \mathbf{n}_F \right]$$

Generalization of stabilized Crouzeix–Raviart methods to non-simplicial meshes. See [Hansbo & Larson, 2003]

The SWIP-ccG method III

- For all interface $F \subset \partial T_1 \cap \partial T_2$ let

$$k_1 := \boldsymbol{\kappa}_{|T_1}\mathbf{n}_F\cdot\mathbf{n}_F, \quad k_2 := \boldsymbol{\kappa}_{|T_2}\mathbf{n}_F\cdot\mathbf{n}_F$$

- Weighted averages to stress the less diffusive side

$$\boxed{\{\varphi\}_\omega := \frac{k_2}{k_1 + k_2}\varphi_{|T_1} + \frac{k_1}{k_1 + k_2}\varphi_{|T_2}}$$

- Harmonic means in penalty term avoids overpenalization

$$\boxed{\gamma_F := \frac{2k_1 k_2}{k_1 + k_2}}$$

Side benefits: Properties of a_h

$$|||v|||^2 := \|\boldsymbol{\kappa}^{1/2}\nabla_h v\|^2_{[L^2(\Omega)]^d} + \sum_{F\in\mathcal{F}_h} \frac{\gamma_F}{h_F}\|[\![v]\!]\|^2_{L^2(F)}$$

Coercivity and boundedness

There exist C_{sta} and C_{bnd} independent of both h and $\boldsymbol{\kappa}$ s.t.

$$\forall v_h \in V_h^{\mathrm{ccg}}, \qquad a_h(v_h, v_h) \geqslant C_{\mathrm{sta}} |||v_h|||^2$$

$$\forall (w, v_h) \in V_{*h} \times V_h^{\mathrm{ccg}}, \qquad a_h(w, v_h) \leqslant C_{\mathrm{bnd}} |||w|||_* |||v_h|||$$

Galerkin orthogonality (with dG paradox)

Provided $u \in V_* := H_0^1(\Omega) \cap H^2(P_\Omega)$,

$$\forall v_h \in V_h^{\mathrm{ccg}}, \qquad a_h(u - u_h, v_h) = \int_\Omega f v_h$$

Side benefits: Error estimates

Error estimate [DP & Ern, 2010]

Assume $u \in H_0^1(\Omega) \cap H^2(P_\Omega)$. There holds

$$|||u - u_h||| \leqslant \left(1 + \frac{C_{\mathrm{bnd}}}{C_{\mathrm{sta}}}\right) \inf_{w_h \in V_h^{\mathrm{ccg}}} |||u - w_h|||_*,$$

with C_{bnd} and C_{sta} independent of both h and $\boldsymbol{\kappa}$.

Convergence rates [DP, 2011]

- $u \in V_* \Rightarrow |||u - u_h||| \leqslant Ch$
- ($\boldsymbol{\kappa}$ homogeneous + ell. reg) $\Rightarrow \|u - u_h\|_{L^2(\Omega)} \leqslant Ch^2$

See [DP & Ern, 2011a] for estimates with $u \in H_0^1(\Omega) \cap H^{1+\alpha}(P_\Omega)$

Convergence to minimal regularity solutions I

- For $F \in \mathcal{F}_h$ the local lifting $\mathrm{r}_F([\![v]\!]) \in \mathbb{P}_d^0(\mathcal{T}_h)^d$ solves

$$\int_\Omega \mathrm{r}_F([\![v]\!]) \cdot \tau_h = \int_F [\![v]\!] \{\tau_h\}_\omega \cdot \mathbf{n}_F \qquad \forall \tau_h \in \mathbb{P}_d^0(\mathcal{T}_h)^d$$

- The counterpart of $\mathfrak{G}_h^{\mathrm{hyb}}$ in ccG methods is

$$\boxed{G_h(v) := \nabla_h v - \sum_{F \in \mathcal{F}_h} \mathrm{r}_F^l([\![v]\!])}$$

$$a_h^{\mathrm{ccg}}(u_h, v_h) = \int_\Omega \kappa G_h(u_h) \cdot G_h(v_h) + s_h(u_h, v_h)$$

Convergence to minimal regularity solutions II

Convergence to minimal regularity solutions [DP, 2011]

Let $(u_h)_{h\in\mathcal{H}}$ denote the sequence of discrete solutions on the admissible mesh family $(\mathcal{T}_h)_{h\in\mathcal{H}}$. Then,

$$\begin{aligned} u_h &\to u && \text{strongly in } L^2(\Omega), \\ \nabla_h u_h &\to \nabla u && \text{strongly in } [L^2(\Omega)]^d, \\ |u_h|_{\mathrm{J}} &\to 0. \end{aligned}$$

with $u \in H^1_0$ unique solution to the continuous problem.

The proof uses the functional analytic results of [DP & Ern, 2010]

Outline

FreeFEM-like implementation in a nutshell I

```
// 1) Define the discrete space
typedef FunctionSpace<span<Polynomial<d, 1> >,
                      gradient<GreenFormula<LInterpolator> >
                      >::type CCGSpace;
CCGSpace Vh(𝒯_h);

// 2) Create test and trial functions
CCGSpace::TrialFunction uh(Vh, "uh");
CCGSpace::TestFunction  vh(Vh, "vh");

// 3) Define the bilinear form
Form2 ah =
  integrate(All<Cell>(𝒯_h),dot(grad(uh),grad(vh)))
 -integrate(All<Face>(𝒯_h),dot(N(),avg(grad(uh)))*jump(vh)
                          +dot(N(),avg(grad(vh)))*jump(uh))
 +integrate(All<Face>(𝒯_h),η/H()*jump(uh)*jump(vh));

// 4) Evaluate the bilinear form
MatrixContext context(A);
evaluate(ah, context);
```

FreeFEM-like implementation in a nutshell II

- Elements of arbitrary shape may be present
- The stencil of local contributions may vary from term to term
- The stencil may be data-dependent (cf. L-construction)
- The stencil may be non-local

- We cannot rely on reference element(s) + table of DOFs
- Instead, global DOF numbering + embedded stencil

Linear combination I

- Let $\mathbb{I} \subset \mathbb{V}_h$ denote the stencil of a discrete linear operator
- A `LinearCombination` $\texttt{lc}^r = (I, \tau_I)_{I \in \mathbb{I}}$ implements

$$\boxed{\texttt{lc}^r(\mathbf{v}_h) = \sum_{I \in \mathbb{I}} \tau_I v_I + \tau_0 \in \mathbb{T}_r}$$

- $r \in \{0, \ldots, 2\}$ denotes the tensor rank of the result
- Algebraic composition of `LinearCombinations` is available

Linear combination II

```
// Cell unknown v_T as a linear combination (I_T is the global DOF number)
LinearCombination<0> vT = Term(I_T,1.);

// Linear combination corresponding to 𝔊_h^grn|_T
LinearCombination<1> GT;
for(F ∈ 𝓕_T)
{
  // Face unknown v_F (possibly resulting from interpolation)
  const LinearCombination<0> & vF = T_h.eval(F);
  GT += |F|_{d-1} / |T|_d (vF-vT) n_{T,F};
}

// Actually perform algebraic operations on coefficients
GT.compact();
```

Figure: Implementation of the Green gradient $\mathfrak{G}_h^{\text{grn}}$

Linear combination III

$$
\begin{aligned}
\texttt{lc}^r &= \texttt{lc}_1^r + \texttt{lc}_2^r \\
&= \sum_{I \in \mathbb{I}_1} \tau_{1,I} v_I + \tau_{1,0} + \sum_{I \in \mathbb{I}_2} \tau_{2,I} v_I + \tau_{2,0} \\
&= \sum_{I \in \mathbb{I}} \tau_I v_I + \tau_0 \quad \text{(compaction)}
\end{aligned}
$$

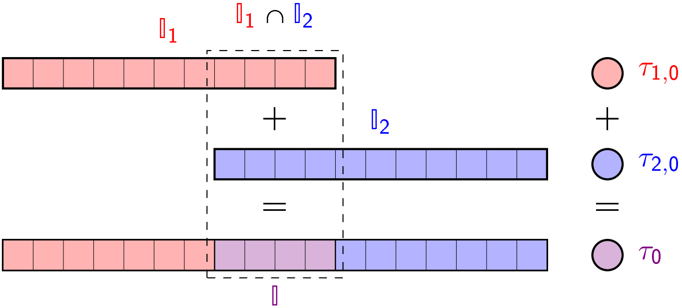

FE-like assembly

- Let $u_h,\ v_h \in V_h^{\mathrm{ccg}}$ and observe that

$$\int_T (\boldsymbol{\kappa}\nabla_h u_h)_{|T}\cdot(\nabla_h v_h)_{|T} \leftrightsquigarrow \left|T\right|_d \, \mathtt{lc}_u\cdot\mathtt{lc}_v$$

$$\leftrightsquigarrow \mathbf{A}_T := \left[\left|T\right|_d \, \tau_{v,I}\cdot\tau_{u,J}\right]_{I\in\mathbb{I},J\in\mathbb{J}}$$

where $\mathtt{lc}_u = (J,\tau_{u,J})_{J\in\mathbb{J}}$ and $\mathtt{lc}_v = (I,\tau_{v,I})_{I\in\mathbb{I}}$

- The assembly step reads

$$\mathbf{A}(\mathbb{I},\mathbb{J}) \leftarrow \mathbf{A}(\mathbb{I},\mathbb{J}) + \mathbf{A}_T$$

The stencils $\mathbb{I}$ and $\mathbb{J}$ replace the table of DOFs!

Outline

The incompressible Navier–Stokes equations

$$
\begin{aligned}
-\nu \triangle u + (u \cdot \nabla) u + \nabla p &= f \quad \text{in } \Omega, \\
\nabla \cdot u &= 0 \quad \text{in } \Omega, \\
u &= 0 \quad \text{on } \partial\Omega, \\
\langle p \rangle_\Omega &= 0.
\end{aligned}
$$

$$
\boxed{U_h := [V_h^{\mathrm{ccg}}]^d, \qquad P_h := \mathbb{P}_d^0(\mathcal{T}_h)/\mathbb{R}}
$$

Find $(u_h, p_h) \in U_h \times P_h$ s.t.

$$
\begin{aligned}
a_h^{\mathrm{ccg}}(u_h, v_h) + t_h(u_h, u_h, v_h) + b_h(v_h, p_h) &= \int_\Omega f \cdot v_h \quad \forall v_h \in U_h \\
-b_h(u_h, q_h) + s_h(p_h, q_h) &= 0 \qquad\qquad \forall q_h \in P_h
\end{aligned}
$$

Pressure-velocity coupling

- The pressure-velocity coupling is realized by the bilinear form

$$b_h(v_h, q_h) := -\sum_{F\in\mathcal{F}_h}\int_F \{v_h\}\cdot\mathbf{n}_F [\![q_h]\!] = -\int_\Omega \mathrm{tr}(G_h(v_h))q_h$$

- Pressure stabilization required for stability

$$s_h(p_h, q_h) := \sum_{F\in\mathcal{F}_h^{\mathrm{i}}}\int_F \frac{h_F}{\nu}[\![p_h]\!][\![q_h]\!], \quad |q_h|_{\mathrm{p}}^2 = s_h(q_h, q_h)$$

Lemma (Stability of the pressure-velocity coupling)

There exists $\beta > 0$ independent of the meshsize h s.t.

$$\forall q_h \in P_h, \qquad \beta\|q_h\|_{L^2(\Omega)} \leqslant \sup_{v_h\in U_h\setminus\{0\}} \frac{b_h(v_h, q_h)}{|\!|\!| v_h |\!|\!|} + \nu^{-\frac{1}{2}}|q_h|_{p}.$$

Implementation

```
// 1) Define the discrete spaces
CCGSpace::VectorTrialFunction uh(d);
CCGSpace::VectorTestFunction vh(d);

// 2) Create test and trial functions
P0Space::TrialFunction ph;
P0Space::TestFunction qh;

// 3) Define the bilinear forms
Range::Index i(Range(0,dim-1));
Form2 ah, bh, sh;
ah = integrate(All<Cell>(𝒯_h),
               sum(i)(dot(grad(uh(i)),grad(vh(i))) ))
    +integrate(Internal<Face>(𝒯_h),
               sum(i)(-dot(fn,avg(grad(uh(i))))*jump(vh(i))
               -jump(uh(i))*dot(N(),avg(grad(vh(i))))
               +η/H()*jump(uh(i))*jump(vh(i))));

bh =-integrate(Internal<Face>(𝒯_h),
               jump(ph)*dot(N(),avg(vh)));

sh = integrate(Internal<Face>(𝒯_h),
               H()*jump(ph)*jump(qh));
```

Convection

- Temam's device for discontinuous approximations
- Non-dissipative formulation
- Asymptotic consistency for smooth/discrete test functions

$$t_h(w,u,v) := \int_\Omega (w\cdot\nabla_h u_i) v_i - \sum_{F\in\mathcal{F}_h^{\mathrm{i}}} \int_F \{w\}\cdot\mathbf{n}_F [\![u]\!]\cdot\{v\}$$
$$+\frac{1}{2}\int_\Omega (\nabla_h\cdot w)(u\cdot v) - \frac{1}{2}\sum_{F\in\mathcal{F}_h}\int_F [\![w]\!]\cdot\mathbf{n}_F\{u\cdot v\}$$

Convergence analysis

Existence [DP & Ern, 2010]

There exists at least one discrete solution $(u_h, p_h) \in X_h$.

Convergence [DP & Ern, 2010, DP, 2011]

Let $((u_h, p_h))_{h \in \mathcal{H}}$ be a sequence of approximate solutions on $(\mathcal{T}_h)_{h \in \mathcal{H}}$. Then, as $h \to 0$, up to a subsequence,

$$\begin{aligned}
u_h &\to u, && \text{in } [L^2(\Omega)]^d, \\
\nabla_h u_h &\to \nabla u, && \text{in } [L^2(\Omega)]^{d,d}, \\
|u_h|_{\mathrm{J}} &\to 0, && \\
p_h &\to p, && \text{in } L^2(\Omega), \\
|p_h|_{\mathrm{p}} &\to 0. &&
\end{aligned}$$

If (u, p) is unique, the whole sequence converges.

A numerical example: The 3d lid-driven cavity problem

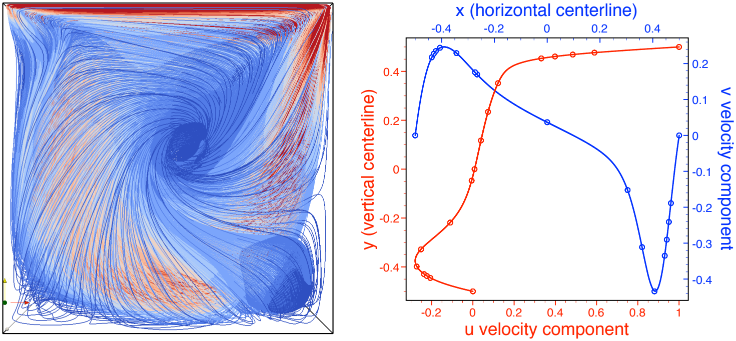

(a) Side view (b) Comparison

Figure: Streamlines and comparison with [Albensoeder *et al.*, 2005]

Further references

- Advection-diffusion [DP, 2010]
- Porous media flow (see Carole Widmer on Friday)
- Elasticity and poromechanics (see Simon Lemaire on Friday)

Daniele A. Di Pietro and Alexandre Ern
Mathematical aspects of discontinuous Galerkin methods
Maths & Applications. Springer–Verlag 2011

Outline

Functional front end

Numerical examples

Function space

- FunctionSpace ↔ incomplete broken polynomial spaces
- Link between algebraic and functional representations

```
FunctionSpace<span</* ... */>,
              gradient</* ... */> >::type Vh;
```

Space	$\mathcal{S}_h$	span	gradient
$\mathbb{P}_d^0(\mathcal{T}_h)$	$\mathcal{T}_h$	Polynomial<d, 0>	Null
V_h^{g}	$\mathcal{P}_h$	Polynomial<d, 1>	GFormula
V_h^{hyb}	$\mathcal{P}_h$	Polynomial<d, 1>	SUSHIFormula<HybridUnknowns>
V_h^{cc}	$\mathcal{P}_h$	Polynomial<d, 1>	SUSHIFormula<LInterpolator>
V_h^{ccg}	$\mathcal{T}_h$	Polynomial<d, 1>	GreenFormula<LInterpolator>

Outline

Functional front end

Numerical examples

- Pure diffusion
- Incompressible Navier–Stokes equations

Pure diffusion I

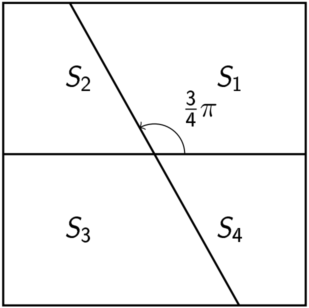

(a) Partition P_Ω

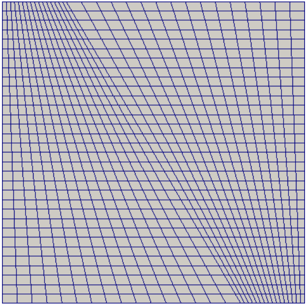

(b) Mesh

Figure: Heterogeneous test cases

Pure diffusion II

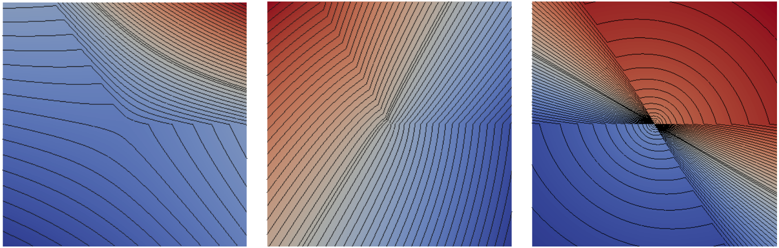

(a) $u \in H^{2.29}(\Omega)$ (b) $u \in H^{1.79}(\Omega)$ (c) $u \in H^{1.29}(\Omega)$

Figure: Low-regularity heterogeneous solutions

Pure diffusion III

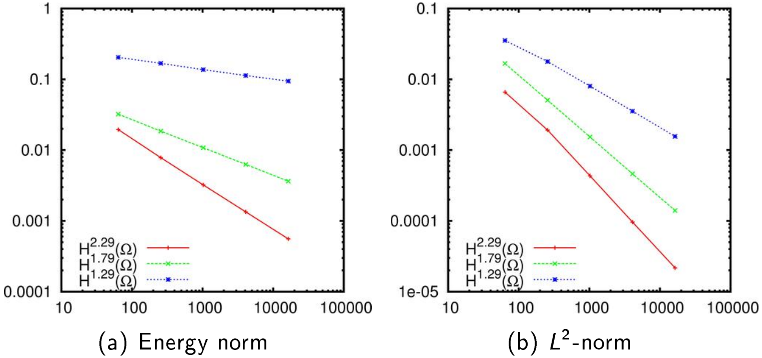

Figure: Optimal convergence

Incompressible Navier–Stokes equations I

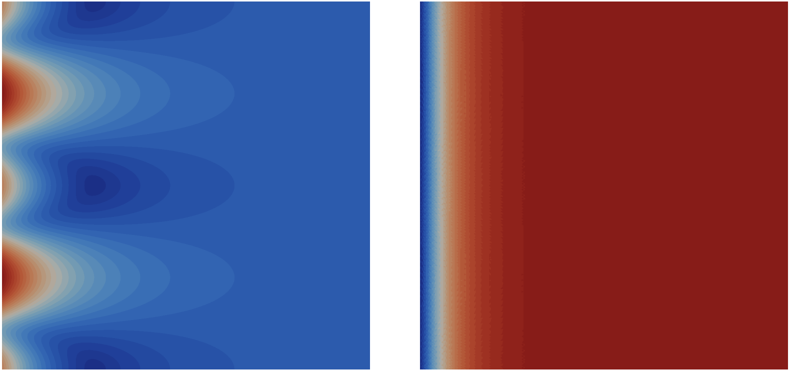

Figure: Kovasznay's problem, velocity magnitude and pressure

Incompressible Navier–Stokes equations II

Table: Convergence results for Kovasznay's problem

$\text{card}(\mathcal{T}_h)$	$\|u - u_h\|_{[L^2(\Omega)]^d}$	ord	$\|p - p_h\|_{L^2(\Omega)}$	ord
224	1.5288e-01	–	2.5693e-01	–
896	4.1691e-02	1.87	1.0847e-01	1.24
3584	1.1115e-02	1.91	4.0251e-02	1.43
14336	2.9261e-03	1.93	1.7487e-02	1.20
57344	7.6622e-04	**1.93**	8.7005e-03	**1.01**

$\text{card}(\mathcal{T}_h)$	$\|\|\|(u - u_h, p - p_h)\|\|\|_{\text{sto}}$	ord
224	4.5730e-01	–
896	2.1185e-01	1.11
3584	1.0319e-01	1.04
14336	5.1495e-02	1.00
57344	2.6540e-02	**0.96**